Vol. 13 (2020) *Acta Physica Polonica B Proceedings Supplement* No 4

NON-EQUILIBRIUM EFFECTS IN THE EVOLUTION OF DARK MATTER*

Andrzej Hryczuk

National Centre for Nuclear Research
Pasteura 7, 02-093 Warsaw, Poland

(Received March 4, 2020)

Among viable dark matter production mechanisms, the thermal freeze-out stands out as the most natural and best motivated one. In the usual theoretical calculations of thermal relic abundance, the assumption of local thermal equilibrium is made. Is this assumption always justified? We discuss more accurate treatments, one relying on the inclusion of higher moments of the Boltzmann equation and the second on solving the evolution of the phase-space distribution function fully numerically.

DOI:10.5506/APhysPolBSupp.13.725

1. Introduction

The production through the thermal freeze-out mechanism remains one of the most natural and attractive ideas to explain the observed present abundance of dark matter (DM) particles. In the standard theoretical approach describing the DM evolution [1], one makes an assumption that the DM is still kept in *local* thermal equilibrium (LTE) with the heat bath during times where annihilations are affecting the DM number density. Here, we address the exceptions to this standard picture, discuss when do they appear and present a method applicable in such cases [2].

As an illustration, we show the impact of departure from LTE on a case study of a generic resonance model, where we find an effect on the DM relic density even up to an order of magnitude. We stress, however, that the methods presented here are of much larger generality and can be applied to other DM models as well.

2. Thermal relic density out of LTE

While the number density is affected by DM annihilation and production processes, the LTE is maintained typically by elastic scatterings of DM

---

* Presented at the $45^{\rm th}$ Congress of Polish Physicists, Kraków, September 13–18, 2019.

on the thermal bath particles. In most cases, the latter processes are expected to have much higher rate than the former, due to mass hierarchy of $m_{\rm DM} \gg m_{\rm SM}$ — for at least some of the Standard Model (SM) states — and, therefore, much higher abundances of said SM states in the thermal bath. At the same time, due to the crossing symmetry (see Fig. 1), the interaction cross section is expected to be of similar order — the argument being that the squared amplitudes for these two diagrams are given by the same analytic function F, only with different kinematics. Unless F varies very strongly with incoming momenta, then indeed the resulting cross sections for elastic scattering and annihilation are numerically very similar.

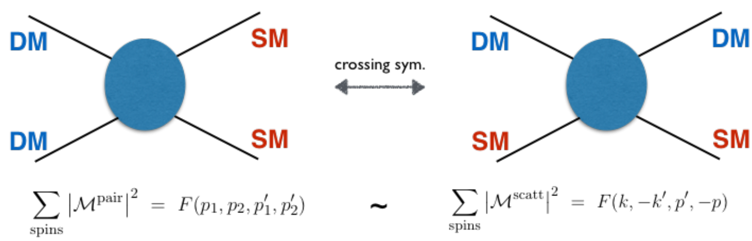

Fig. 1. Diagrammatic relation between DM annihilation and elastic scattering of DM on SM states.

However, there are important exceptions to the above argument. In general, one can delineate three classes of such cases:

- Strong dependence of annihilation or scattering process on the kinematics, *e.g.*, in the presence of (narrow) resonances.
- Violation of $m_{\rm DM} \gg m_{\rm SM}$ hierarchy, *e.g.*, by sub-threshold annihilation.
- Annihilation and scattering processes having different origin, *e.g.*, in the case of semi-annihilation [3] models[1].

In [2], both semi-analytic and fully numerical methods were developed to solve the Boltzmann equation and to compute the DM relic abundance in such circumstances, which we briefly review below.

[1] Note that also in models where the dark sector contains more states than only the DM particle, one can expect that not every particle is in LTE. Indeed, even in simple co-annihilation scenarios some states, *e.g.*, the bino in supersymmetric models, can be so weakly coupled that their distribution can be far from the equilibrium one.

2.1. The coupled Boltzmann equations (cBE)

The evolution of the DM phase-space density $f_{\rm DM}(t,\boldsymbol{p})$ is well-described by the Boltzmann equation of the form of

$$E\left(\partial_t - H\boldsymbol{p}\cdot\nabla_{\boldsymbol{p}}\right) f_{\rm DM} = C[f_{\rm DM}]\,, \tag{1}$$

where H is the Hubble parameter and the collision term $C[f_{\rm DM}]$ contains all interactions between DM and SM particles, in particular annihilation

$$C_{\rm ann} = g_{\rm DM}E\int\frac{{\rm d}^3\tilde{p}}{(2\pi)^3}\,v\sigma_{\bar{\rm DM}\,{\rm DM}\to\bar{f}f}\left[f_{\rm DM}^{\rm eq}(E)f_{\rm DM}^{\rm eq}\left(\tilde{E}\right) - f_{\rm DM}(E)f_{\rm DM}\left(\tilde{E}\right)\right]\,, \tag{2}$$

and elastic scatterings [2, 4, 5]

$$C_{\rm el} \simeq \frac{E}{2}\gamma(T)\left[TE\partial_p^2 + \left(p + 2T\frac{E}{p} + T\frac{p}{E}\right)\partial_p + 3\right] f_{\rm DM}\,, \tag{3}$$

where $v = (E\tilde{E})^{-1}[(p\cdot\tilde{p})^2 - m_{\rm DM}^4]^{1/2}$, the scattering term is given under the assumption of momentum transfer much smaller than the DM mass, and the momentum exchange rate is obtained from transfer cross section $\sigma_{\rm T}$ by

$$\gamma(T) \equiv \frac{1}{3\pi^2 g_{\rm DM} m_{\rm DM}}\int {\rm d}\omega\, g^{\pm}\partial_\omega\left(k^4\sigma_{\rm T}(k)\right)\,. \tag{4}$$

In analogy to $Y \equiv n_{\rm DM}/s$ for the zeroth moment of $f_{\rm DM}$, we define dimensionless variable for its *second* moment [2, 4]

$$y \equiv \frac{m_{\rm DM}}{3s^{2/3}}\left\langle\frac{\boldsymbol{p}^2}{E}\right\rangle = \frac{m_{\rm DM}}{3s^{2/3}}\frac{g_{\rm DM}}{n_{\rm DM}}\int\frac{{\rm d}^3p}{(2\pi)^3}\frac{\boldsymbol{p}^2}{E}f_{\rm DM}(\boldsymbol{p})\,. \tag{5}$$

If DM particles follow the Maxwell–Boltzmann distribution, *e.g.*, due to sufficiently strong self-scatterings, they have a *temperature* $T_{\rm DM} = ys^{2/3}/m_{\rm DM}$. In general, for non-thermal distributions, one can read the above equation as a *definition* of DM 'temperature', in terms of the $2^{\rm nd}$ moment of $f_{\rm DM}$.

Integrating Eq. (1) over $g_{\rm DM}\int {\rm d}^3p/(2\pi)^3/E$ and $g_{\rm DM}\int {\rm d}^3p/(2\pi)^3\boldsymbol{p}^2/E^2$, respectively, one arrives at the system of cBEs

$$\frac{Y'}{Y} = \frac{sY}{x\tilde{H}}\left[\frac{Y_{\rm eq}^2}{Y^2}\langle\sigma v\rangle - \langle\sigma v\rangle_{\rm neq}\right], \tag{6}$$

$$\begin{aligned}\frac{y'}{y} &= \frac{\gamma(T)}{x\tilde{H}}\left[\frac{y_{\rm eq}}{y} - 1\right] + \frac{sY}{x\tilde{H}}\left[\langle\sigma v\rangle_{\rm neq} - \langle\sigma v\rangle_{2,{\rm neq}}\right] \\ &\quad + \frac{sY}{x\tilde{H}}\frac{Y_{\rm eq}^2}{Y^2}\left[\frac{y_{\rm eq}}{y}\langle\sigma v\rangle_2 - \langle\sigma v\rangle\right] + \frac{H}{x\tilde{H}}\frac{\langle p^4/E^3\rangle}{3T_{\rm DM}}\,,\end{aligned} \tag{7}$$

where, in addition to $\langle \sigma v \rangle$, we also need to define

$$\langle \sigma v \rangle_2 \equiv \frac{g_{\mathrm{DM}}^2}{T n_{\mathrm{DM,eq}}^2} \int \frac{\mathrm{d}^3 p \, \mathrm{d}^3 \tilde{p}}{(2\pi)^6} \frac{p^2}{3E} \sigma v_{\bar{\mathrm{DM}}\,\mathrm{DM} \to \bar{f} f} f_{\mathrm{DM,eq}}(\boldsymbol{p}) f_{\mathrm{DM,eq}}(\tilde{\boldsymbol{p}}) \,. \quad (8)$$

The above set of cBEs governs the evolution of an equilibrium DM phase-space distribution but at a temperature different from that of the heat bath[2].

2.2. The full phase-space Boltzmann equation (fBE)

The second method applicable even if LTE is not maintained around freeze-out is to solve the Boltzmann Eq. (1) at the full phase-space density level. We start by rewriting it in two dimensionless coordinates $x(t,p) \equiv m_{\mathrm{DM}}/T$ and $q(t,p) \equiv p/T$, where q is now the 'momentum' coordinate that depends on both p and t. Such new coordinates absorb the change of the DM momentum and density due to the Hubble expansion.

We then discretize the variable q into q_i with $i \in \{1, \ldots, N\}$ what allows to rewrite the initial *integro partial differential equation* into a set of N coupled ODEs

$$\begin{aligned} \frac{\mathrm{d}}{\mathrm{d}x} f_i = & \frac{m_{\mathrm{DM}}^3}{\tilde{H} x^4} \frac{g_{\bar{\mathrm{DM}}}}{2\pi^2} \sum_{j=1}^{N-1} \frac{\Delta \tilde{q}_j}{2} \Big[\tilde{q}_j^2 \left\langle v \sigma_{\bar{\mathrm{DM}}\,\mathrm{DM} \to \bar{f} f} \right\rangle_{i,j}^{\theta} \left(f_i^{\mathrm{eq}} f_j^{\mathrm{eq}} - f_i f_j \right) \\ & + \tilde{q}_{j+1}^2 \left\langle v \sigma_{\bar{\mathrm{DM}}\,\mathrm{DM} \to \bar{f} f} \right\rangle_{i,j+1}^{\theta} \left(f_i^{\mathrm{eq}} f_{j+1}^{\mathrm{eq}} - f_i f_{j+1} \right) \Big] \\ & + \frac{\gamma(x)}{2\tilde{H} x} \left[x_{q,i} \partial_q^2 f_i + \left(q_i + \frac{2 x_{q,i}}{q_i} + \frac{q_i}{x_{q,i}} \right) \partial_q f_i + 3 f_i \right] + \tilde{g} \frac{q_i}{x} \partial_q f_i \,, \end{aligned} \quad (9)$$

where $f_i \equiv f_{\mathrm{DM}}(x, q_i)$, and the derivatives $\partial_q f_i$ and $\partial_q^2 f_i$ are determined numerically from several neighboring points to f_i, θ is the angle between $\boldsymbol{q}$ and $\tilde{\boldsymbol{q}}$, and $x_q \equiv \sqrt{x^2 + q^2}$. $\langle v \sigma_{\bar{\mathrm{DM}}\,\mathrm{DM} \to \bar{f} f} \rangle_{i,j}^{\theta}$ is the velocity-weighted cross section averaged over θ and $\Delta \tilde{q}_j \equiv \tilde{q}_{j+1} - \tilde{q}_j$.

[2] The set of cBEs (6) and (7) includes a higher moment of f_{DM}, and hence does not close w.r.t. the variables Y and y. We need additional input to determine the quantities $\langle \sigma v \rangle_{\mathrm{neq}}$, $\langle \sigma v \rangle_{2,\mathrm{neq}}$ and $\langle p^4/E^3 \rangle$ in terms of only y and Y. We accomplish this by making the following Ansatz for these quantities [2]:

$$\begin{aligned} \langle \sigma v \rangle_{\mathrm{neq}} &= \langle \sigma v \rangle \big|_{T = y s^{2/3}/m_{\mathrm{DM}}} \,, \qquad \langle \sigma v \rangle_{2,\mathrm{neq}} = \langle \sigma v \rangle_2 \big|_{T = y s^{2/3}/m_{\mathrm{DM}}} \,, \\ \langle p^4/E^3 \rangle &= \left[\frac{g_{\mathrm{DM}}}{2\pi^2 n_{\mathrm{DM,eq}}(T)} \int \mathrm{d}p \, \frac{p^6}{E^3} \mathrm{e}^{-\frac{E}{T}} \right]_{T = y s^{2/3}/m_{\mathrm{DM}}} . \end{aligned}$$

3. Case study: resonant annihilation

The above formalism was developed in [2] and applied there to the scalar singlet DM model featuring SM Higgs resonance. Here, we show the result for its generalization to an arbitrary resonant annihilation of scalar DM annihilating through s-channel scalar resonance into fermion pair. The model can be effectively parametrized by the resonance width (γ), distance to the peak (δ) and the coupling factor (ρ), all defined below. In $2 \to 2$ processes, the amplitude is dimensionless. Therefore, for resonant processes of the type $\mathrm{DM\,DM} \to R \to XX$, amplitude can depend only on these three parameters and one mass ratio, which we will choose to be m_X/m_{DM}. It follows that the cross section is a function of 5 parameters

$$m_{\mathrm{DM}}\,, \qquad \mu = \frac{m_X}{m_{\mathrm{DM}}}\,, \qquad \gamma = \frac{\Gamma}{m_{\mathrm{R}}}\,, \qquad \delta = \frac{4m_{\mathrm{DM}}^2}{m_{\mathrm{R}}^2} - 1\,, \qquad \rho = (\lambda g)^2\,. \tag{10}$$

The latter, ρ, is not specified explicitly in what follows as it is always fixed by the relic density constraint for a given parameter point. The relevant amplitudes are given by

$$\left|\hat{\mathcal{M}}_{\mathrm{ann}}\right|^2 = \frac{1}{2}\frac{\tilde{s}(1+\delta)^2\left(1-\frac{4m_X^2}{s}\right)}{\left[\tilde{s}(1+\delta)^2-1\right]^2+\gamma^2}\,, \qquad \left|\hat{\mathcal{M}}_{\mathrm{scatt}}\right|^2 = \frac{1}{2\mu^2}\frac{1-\tilde{t}}{\left(\tilde{t}-\frac{1}{(1+\delta)\mu^2}\right)^2}\,, \tag{11}$$

where $\tilde{s}$ and $\tilde{t}$ are Mandelstam variables normalized by $4m_{\mathrm{DM}}^2$.

The results for the effect of departure from LTE are shown in Fig. 2. The contours and colors show the ratio of relic abundance with cBE ($\Omega h^2_{\mathrm{cBE}}$) to the result from standard treatment (Ωh_0^2) in the (δ, γ) plane. Well outside the resonance region or for large widths, the cBE leads to identical results as the standard approach, indicating that in that cases the assumption of LTE during chemical freeze-out is well-satisfied. Near the resonance at zero-velocity ($\delta \sim 0$) or in the region where the resonant $\tilde{s}$ coincides with the typical velocities during freeze-out ($\delta \in [-0.4, -0.1]$), one can see a large difference between the two treatments, implying that the LTE assumption must be strongly violated. Note that the effect is significantly larger than observational uncertainty on Ωh^2 for a wide range of parameters, in particular for widths potentially as large as the Z boson one.

The results above are obtained with the cBE method which provides a very good description for the final DM abundance, capturing most of the effect of the kinetic decoupling. Nevertheless, for high-precision results, one needs to actually solve the full Boltzmann equation in phase space. This is because, as the full numerical solution reveals, the shape of $f_{\mathrm{DM}}(t,\boldsymbol{p})$

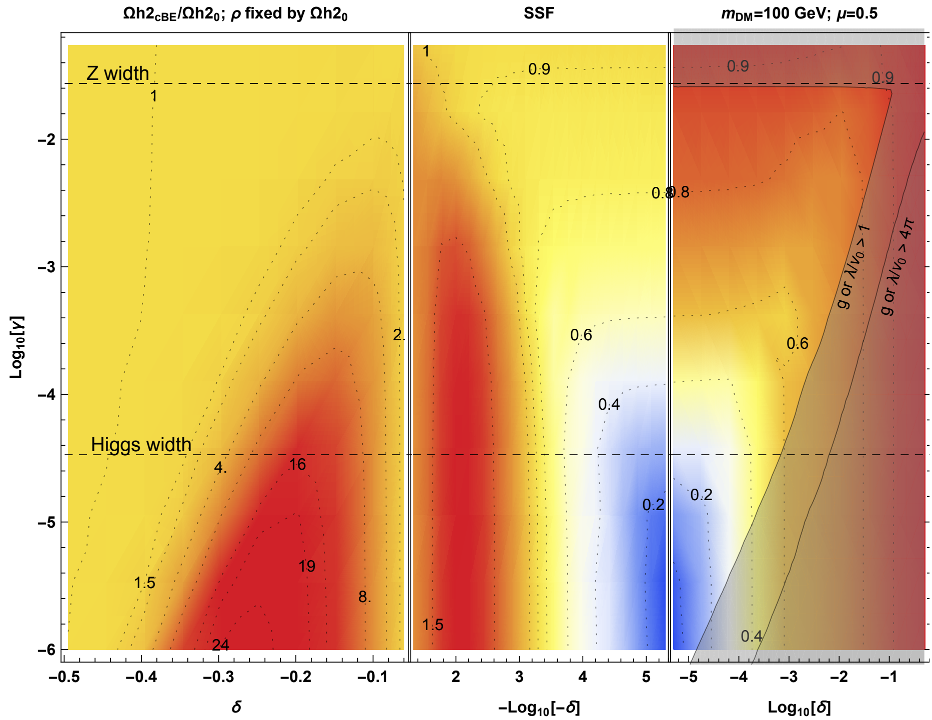

Fig. 2. (Color online) The effect of LTE violation on the DM relic density for scalar DM resonance model annihilating into SM fermions for $m_{\rm DM} = 100$ GeV and $\mu = 0.5$. The contours show the value of $\Omega h^2_{\rm cBE}/\Omega h^2_0$. The gray shaded area on the right is where the couplings for this model grow large enough to violate unitarity.

can be quite different from the Maxwell–Boltzmann form, which can introduce departure from the assumptions used in the cBEs. As an example, in Fig. 3, the time snapshots of the evolution of $f_{\rm DM}(t,\boldsymbol{p})$ just before, during and at the end of freeze-out are shown. The top panels show normalized $p^2 f_{\rm DM}(t,\boldsymbol{p})$ at the $T_{\rm DM}$ for the actual (blue) and equilibrium (black) shapes. The lower panels show evolution of y for the actual (solid/blue) and LTE (dashed/black) cases, where the dot indicates the time of the snapshot. As it is evident, the shape of the distribution can indeed depart from equilibrium one, which can have either a noticeable impact on the result for the relic density or a modest one depending on whether or not the shape during chemical freeze-out is affected for momenta that can combine to $\sqrt{s} \sim m_{\rm R}$.

Finally, let us comment on applications to other, non-resonant, models. In [6], we studied the semi-annihilation in the $\mathbb{Z}_3$ singlet dark matter. To this end, the formalism presented above had to be extended to the semi-annihilation processes, which significantly increases the numerical complex-

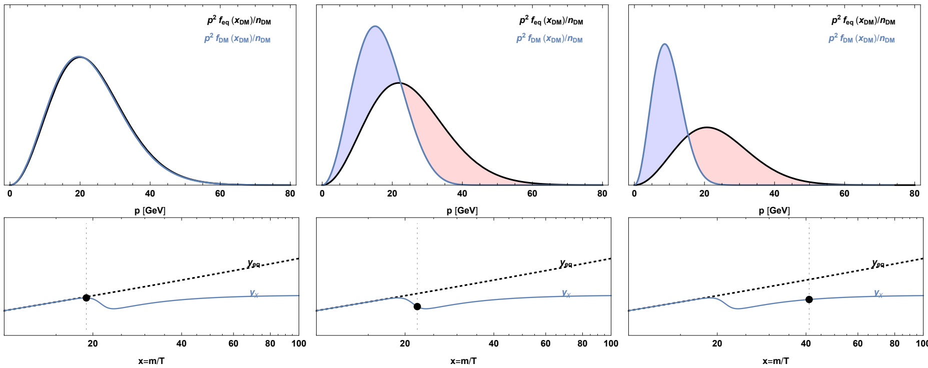

Fig. 3. (Color online) The evolution of $f_{\rm DM}(t,\boldsymbol{p})$ for the SSF model, $m_{\rm DM} = 58$ GeV, $\gamma = 3.4\times10^{-5}$ and $\delta = -0.143$.

ity of the problem. There, it has also been found that the $T_{\rm DM}$ can differ significantly from $T_{\rm SM}$, but the effect on the relic density was mild, due to relatively velocity independent annihilation process in the $\mathbb{Z}_3$ model. This is expected to change for slightly more complicated scenarios, based on $\mathbb{Z}_N$ symmetry or more involved scalar sector [7]. And last, but not least, study of other cases with both cBE and fBE methods like the aforementioned sub-threshold annihilation and the late kinetic decoupling with the Sommerfeld enhanced annihilation is a subject of ongoing work [8].

4. Conclusions

The departure from LTE can have significant implications for the evolution of DM density and relic abundance. We discussed two methods for calculating this effect: one introducing a coupled system of equations for DM density and temperature, and second relying on numerically solving for the full $f_{\rm DM}(t,\boldsymbol{p})$. We also discussed applications of the formalism and presented exemplary results in a case study of a generic resonance DM model.

I would like to thank Tobias Binder, Torsten Bringmann, Michael Gustafsson, Andi Hektor and Kristjan Kannike for joint work on the projects presented in this paper. This work was supported by the National Science Centre, Poland (NCN), research grant No. 2018/31/D/ST2/00813.

REFERENCES

[1] P. Gondolo, G. Gelmini, *Nucl. Phys. B* **360**, 145 (1991).

[2] T. Binder, T. Bringmann, M. Gustafsson, A. Hryczuk, *Phys. Rev. D* **96**, 115010 (2017).

[3] F. D'Eramo, J. Thaler, *J. High Energy Phys.* **1006**, 109 (2010).

[4] T. Bringmann, S. Hofmann, *J. Cosmol. Astropart. Phys.* **0704**, 016 (2007).

[5] T. Binder *et al.*, *J. Cosmol. Astropart. Phys.* **1611**, 043 (2016).

[6] A. Hektor, A. Hryczuk, K. Kannike, *J. High Energy. Phys.* **1903**, 204 (2019).

[7] N. Benincasa, A. Hektor, A. Hryczuk, K. Kannike, work in progress.

[8] T. Binder, T. Bringmann, M. Gustafsson, A. Hryczuk, work in progress.